Applied Energy 112 (2013) 1171–1180

Contents lists available at SciVerse ScienceDirect

Applied Energy

journal homepage: www.elsevier.com/locate/apenergy

Theoretical analysis of a thermoelectric generator using exhaust gas of vehicles as heat source

Yuchao Wang [a,b], Chuanshan Dai [a,b], Shixue Wang [a,c,*]

[a] School of Mechanical Engineering, Tianjin University, China
[b] Key Laboratory of Efficient Utilization of Low and Medium Grade Energy, MOE, Tianjin University, China
[c] State Key Laboratory of Engines, Tianjin University, China

HIGHLIGHTS

- Presents a mathematical model of TEG and preliminary analysis of factors.
- Effects of heat transfer coefficients of two sides of TEG are different.
- With the change of height of PN couple, there is a peak value of output power.
- Exists a maximum which appears when external resistance is bigger.
- We try to use phase-change material to reform our experiment design.

ARTICLE INFO

Article history:
Received 25 September 2012
Received in revised form 29 December 2012
Accepted 3 January 2013
Available online 23 February 2013

Keywords:
Vehicle exhaust gas
Thermoelectric
Output power
Convection heat transfer coefficient
Design optimization

ABSTRACT

Based on Fourier's law and the Seebeck effect, this paper presents a mathematical model of a Thermoelectric Generator (TEG) device using the exhaust gas of vehicles as heat source. The model simulates the impact of relevant factors, including vehicles exhaust mass flow rate, temperature and mass flow rate of different types of cooling fluid, convection heat transfer coefficient, height of PN couple, the ratio of external resistance to internal resistance of the circuit on the output power and efficiency. The results show that the output power and efficiency increase significantly by changing the convection heat transfer coefficient of the high-temperature-side than that of low-temperature-side. The results also show that with variation in the height of the PN couple, the output power occur a peak value, and the peak value decreases when decreasing the thermal conductivity of the PN couple, and increases when increasing the Seebeck coefficient and electric conductivity of the material. Meanwhile, a maximum output power and efficiency of a TEG appear when external resistance is greater than internal resistance. This is different from a common circuit, and with the increment of *ZT*, the maximum value moves toward the direction of an increasing ratio of external resistance to internal resistance. Finally, we propose a new idea to reform our experiment design to achieve better performance.

1. Introduction

Transportation vehicles powered by combustion engines are one of the significant causes for the petro fuel crisis and intensifying environment pollution. From the perspective of the energy balance of a combustion engine, the power efficiency accounts for only 30–45% of the total amount of heat generated by the fuel used. The rest of the energy, except for a 10% or less loss to overcome friction, is not fully used. It is mainly emitted to the atmosphere through heat dissipation and circuit cooling exhaust. During this process, 40% of the energy is lost through gas emission waste [1]. Capturing a small portion of the available energy with thermoelectric devices can reduce engine loads and/or alternator size thus decreasing pollutant emissions and fuel consumption [2]. Thermoelectric devices can also be used in conjunction with traditional CO_2 reduction approaches (reducing friction, decreasing pumping losses, and improving combustion efficiency) to further reduce greenhouse gas emissions [3]. Previous studies had estimated that if the amount of driving energy required for the production of electrical power (approximately 6%), could be recovered, this would result in an overall reduction of fuel consumption by 10% [4]. It makes sense that recycling and reusing waste exhaust gas can not only enhance fuel energy use efficiency, but also reduce air pollution. Thermal power technology such as the TEG arouses, therefore, significant attention worldwide. TEG is a technology for directly converting thermal energy into electrical energy. It has no moving

* Corresponding author at: School of Mechanical Engineering, Tianjin University, China.
E-mail address: wangshixue_64@tju.edu.cn (S. Wang).

0306-2619/$ - see front matter © 2013 Elsevier Ltd. All rights reserved.
http://dx.doi.org/10.1016/j.apenergy.2013.01.018

Nomenclature

Abbreviation

TEG	Thermoelectric Generator
MPPT	maximum power point tracking

Symbols

r	row
m	line
n	total number of PN couples
T	temperature (°C)
q	quantity of heat (W)
S	Seebeck coefficient (μV/K)
λ	thermal conductivity (W/(mK))
A	cross sectional area (m^2)
s	cross sectional area of one kind of material in one unit (m^2)
σ	electrical conductivity (s/m)
H	height of either P or N thermoelectric materials (m)
ρ	electric resistivity (Ωm)
K	thermal conductance (W/K)
R_1	internal resistance (Ω)
R_2	external resistance (Ω)
h	convective heat transfer coefficient (W/(m^2 K))
C	specific heat capacity (kJ/(kg°C))
M	mass flow rate (g/s)
P	output power (W)
η	efficiency (%)

Subscript

f	exhaust
c	cooling fluid
1	hot side
2	cold side
p	P material
n	N material
i	in
o	out
y	y direction
overall	total

Superscript

j	jth unit

parts, is compact, quiet, highly reliable and environmentally friendly. Because of these merits, it is presently becoming a noticeable research direction [5]. Several years ago, some car manufacturers, such as HI-Z in the USA, Nissan in Japan, BMW in Germany, had successfully developed a thermoelectric engine to recycle vehicle exhaust gas. However, the quantity of heat recycled is quite limited; in general less than 5%. This is somewhat limited by thermoelectric materials. Although challenges exist, it may be possible to recover significant amounts of exhaust waste heat with thermoelectric devices, particularly as research of materials and application of heat transfer technologies continue to improve the performance of these elements. Continued research in this area is further encouraged as China's current national goal and the US Department of Energy's commitment to reducing America's dependence on foreign oil gathers more attention [6].

With the rapid development of semiconductor technology and the growing crisis of decreasing fossil fuel, more and more attention has been drawn to this area. But, what we must emphasize is that heat recovery efficiencies are still low now, both on a system basis (<2.5%) and on a thermoelectric generator basis (<3.5%), despite great progress made over the last decade in the thermoelectric materials figure of *ZT* merit values [7]. The figure of merit value is a non-dimensional number that provides an overall assessment of the thermo-element's electrical conversion efficiency. Although material selection and *ZT* values are important to the performance of the thermoelectric generator, power output also greatly depends on the availability of heat in order to maintain a large temperature difference between the hot and cold side of the materials element [7]. Bell [8] pointed out two important pathways that would lead to additional applications of thermoelectric (TE) devices. One is to promote the intrinsic efficiencies of TE materials. From the standpoint of current new thermoelectric materials research and development, a large number of studies concerning thermoelectricity focus on how to improve heat-to-electricity conversion efficiency of thermoelectric materials; that is, how to improve the thermoelectric *ZT* figure of merit of these materials. Nanotechnology [9,10], novel technology in solid state physics and semiconductor physics [11,12] is employed to explore this exciting field. Another approach is to improve the way existing TEGs are currently used. In addition to the research of thermoelectric materials, reasonable thermal design and management of the thermoelectric generator is equally important for improving generating performance [13]. The key factor should be the usage of economical and efficient of heat sources. From the perspective of system analysis and optimization, Rowe and Gao [14] provided a practical procedure for optimizing TEG module geometry guided by the "economic factor". Gou et al. [5] tested results, and discussions showed the promising potential of using a thermoelectric generator for low-temperature waste heat recovery, especially in the industrial field. More than 2% efficiency is achieved, increasing slightly with a boost of temperature difference. Hsu et al. [15] proposed a concept of "effective Seebeck coefficient", which discussed the inconsistency between the theoretical Seebeck coefficient and the measured one. Applying an appropriate pressure on a TEG module was suggested to improve performance. Bismuth telluride material was used in their experiment to verify their conclusion. Liang et al. [16] also constructed an analytical model of a parallel TEG by theoretical analysis, to investigate how contact effect reduces the output power of a parallel TEG and, further, to verify the model by experimental testing. Hsiao et al. [17] had constructed a one-dimensional thermal resistance model, and the results were verified by experiments. The model results showed that a TEG module presented better performance on the exhaust pipe than on radiator. Kim [18] had also proposed an experimental method to extract the intrinsic and extrinsic Seebeck coefficients and resistances of a TEG. Crane and Bell [19] had studied the influence by changing the temperature of exhaust gas and the mass flow rate experimentally, and gave an optimizing method. Eakburanawat and Boonyaroonate [20] described a thermoelectric battery charger powered by thermoelectric (TE) power modules. It might not be economical initially, but the results derived here may lay a foundation for further investigations of TE battery charger systems. Yu and Chau [1] had combined MPPT and Ćuk converter technology with a TEG device, and achieved 20% improvement in performance. Espinosa [21] had proposed an idea that connected different PN materials that had different "best working temperature ranges" in order to realize the effect of temperature gradient optimization, and to get a better performance. He also tested the thermoelectric performance of many kinds of materials'. Chen et al. [22,23] also

explored the performance of the TEG with multi-element thermoelectric equipment and built a model of a two-stage semiconductor thermoelectric-generator with external heat-transfer. Multi-stage models consist of different temperatures, such as low, medium, and high. Thermoelectric modules were also proposed by other scholars, such as Xiao et al. [13,24] and Chen et al. [23]. Their results showed that reasonable thermal design of a thermoelectric module could take full advantage of the characteristics of each thermoelectric material and effectively improved the performance of power generation.

Several authors had demonstrated the use of thermoelectric elements for automobile heat recovery, installing the devices in the vehicle exhaust [25–28]. Hsu et al. [29,30], Masahide et al. [31], Yodovard [32], Yu and Chau [33], Xu et al. [34], Gou et al. [5], and Suter et al. [35] applied thermoelectric generation technology to environmentally-friendly vehicles. Both waste heats from vehicle exhaust and engine were converted into electrical power to provide auxiliary power for the vehicle. To achieve better performance or efficiency, many scholars designed various kinds of integrated systems, such as combining with photovoltaic [36,37] or Organic Rankine Cycles (ORCs) [38]. Many scholars also studied thermoelectric cooling technology to cool important vehicle devices, or for comfort [39–42]. Most existing researches are experiments with low-and-medium temperature heat sources, or analyzing the influence of external conditions such as temperature and mass flow rate of both cold and heat sources. However, theory research and internal optimization of TEG devices and other related contents is far less. It is noticed that the exhaust gas temperature is not constant, in fact, reducing along with the TEG. The temperature profile inside the TEG module and its changing behavior is important for designing a thermoelectric device. If the inlet temperature profile of the device can be achieved, it can provide great help to optimize the device and to analyze the influence of various factors. To this end, a simple thermodynamic model is proposed that can be used to calculate the temperature profile in the TEG module, and to theoretically predict output power and efficiency. The effects of various factors on the performance of a TEG also have been analyzed.

2. Mathematical model

Thermoelectric Generator (TEG) device consists of many small couples of P type and N type thermoelectric materials assembled according to definite permutations and combinations. Completely symmetrical device fluctuation is assumed, regardless of parts studied, as shown in Fig. 1. We start our study from a single PN unit considered to have the same length scale. The entire TEG, therefore, can be divided into many small units. The outlet temperatures of the former unit are treated as the inlet temperatures for the next unit; thus the calculation can be done continuously. Some assumptions are made as follows:

(1) Steady state in thermal and flow.
(2) The thermal resistance of copper chip is ignored, as it is quite small.
(3) The gas in the gaps is ignored.
(4) No contact thermal resistance.
(5) Heat conduction is perpendicular to flow direction, the heat conduction in the axial direction is omitted, and the heat radiation is also omitted.
(6) The thermal conductivity of the PN unit is constant.
(7) Thomason heat is ignored.
(8) It has r rows and each row has m couples, so the total number of PN couples, n, can be defined as $n = r \cdot m$. PN couples are connected in series. We assume the materials of each row are exactly the same, so performance of each row can be the same. We can simplify the three-dimensional model into a two-dimension model.

As shown in Fig. 1, the TEG works between a heat source (exhausted gas) and cold source (ambient air). The heat is transferred from the heat source at temperature of T_f, and released at temperature of T_c. In this process, part of the heat is converted into electricity that is transmitted in a form of output power or electromotive force.

In the present model, the Seebeck effect and Fourier's law of heat conduction are assumed to be dominated in a representative size of unit as shown in Fig. 1. In the j unit, the energy conservation equations, including P and N type materials, can be given. Assuming T_1^j be the averaged temperature of the hot side of one unit length in the axial direction, the heat transfer rates (in y direction) through each branch of PN type thermoelectric materials q_{p1}^j andq_{n1}^j at the root side, respectively, can be expressed as:

$$q_{p1}^j = S_{p1}^j I T_1^j - \lambda_{py}^j A_p \left.\frac{dT}{dy}\right|_{y=0} \tag{1}$$

$$q_{n1}^j = -S_{n1}^j I T_1^j - \lambda_{ny}^j A_n \left.\frac{dT}{dy}\right|_{y=0} \tag{2}$$

Let T_2^j be the averaged temperature of the cold side of one unit at the outer end of $y = H$; the heat transfer rates through the PN thermoelectric materials q_{p2}^j and q_{n2}^j, respectively, can be expressed as:

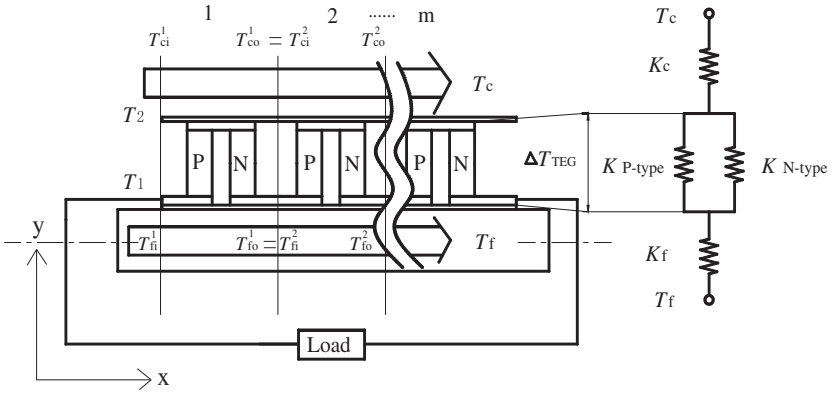

Fig. 1. A schematic diagram of the theoretic model.

$$q_{p2}^j = S_{p2}^j I T_2^j - \lambda_{py}^j A_p \left.\frac{dT}{dy}\right|_{y=H} \tag{3}$$

$$q_{n2}^j = -S_{n2}^j I T_2^j - \lambda_{ny}^j A_n \left.\frac{dT}{dy}\right|_{y=H} \tag{4}$$

where S^j is the Seebeck coefficient, I is the output current, λ_y^j is the thermal conductivity of the y direction of P or N type thermoelectric materials; $A_p(A_n)$ is the cross sectional area of a unit of P or N type thermoelectric materials; dT/dy is the temperature gradient; H is the height of either P or N thermoelectric materials. The relationship between the temperature gradient with joule heat per unit height in PN couples is given by:

$$-\lambda_{py}^j A_p \frac{d^2T}{dy^2} = \frac{I^2 \rho_p^j}{A_p} \tag{5}$$

$$-\lambda_{ny}^j A_n \frac{d^2T}{dy^2} = \frac{I^2 \rho_n^j}{A_n} \tag{6}$$

where ρ^j is the electric resistivity of the material.

The boundary conditions are given by:

$$y = 0; \quad T = T_1^j \tag{7}$$

$$y = H; \quad T = T_2^j \tag{8}$$

From (3–6), we derive:

$$\lambda_{py}^j A_p \frac{dT}{dy} = \frac{I^2 \rho_p^j (y - H/2)}{A_p} + \frac{\lambda_{py}^j A_p \left(T_2^j - T_1^j\right)}{H} \tag{9}$$

$$\lambda_{ny}^j A_n \frac{dT}{dy} = \frac{I^2 \rho_n^j (y - H/2)}{A_n} + \frac{\lambda_{ny}^j A_n \left(T_2^j - T_1^j\right)}{H} \tag{10}$$

Eq. (9) together with Eqs. (1), (2), and (10) together with Eq. (3), (4), the unit absorbed heat $q_1^j(y = 0)$ and unit released heat $q_2^j(y = H)$ in j unit can be obtained:

$$q_1^j = \left(S_{p1}^j - S_{n1}^j\right) I T_1^j + K\left(T_1^j - T_2^j\right) - I^2 R_1^j/2 \tag{11}$$

$$q_2^j = \left(S_{p2}^j - S_{n2}^j\right) I T_2^j + K\left(T_1^j - T_2^j\right) + I^2 R_1^j/2 \tag{12}$$

where

$$K^j = \frac{\lambda_{py}^j A_p}{H} + \frac{\lambda_{ny}^j A_n}{H}, \quad R_1^j = \frac{\rho_p^j H}{A_p} + \frac{\rho_n^j H}{A_n}$$

K^j is the thermal conductance of j unit; R_1^j is the electric resistance of j unit of PN couple.Note that the absorbed heat at the hot side q_1^j from exhaust gas can also be written as:

$$q_1^j = h_1 A_1^j \left(\frac{t_{fi}^j + t_{fo}^j}{2} - T_1^j\right) \tag{13}$$

Similarly, the released heat q_2^j at the cold side to ambient air can also be written as:

$$q_2^j = h_2 A_2^j \left(T_2^j - \frac{t_{co}^j + t_{ci}^j}{2}\right) \tag{14}$$

where A_1^j, A_2^j are the heat exchange areas of the hot side and cold side in the j unit, respectively. h_1 is the convective heat transfer coefficient of the hot side; h_2 is convective heat transfer coefficient of the cold side.

So the following equations can be obtained:

$$h_1 A_1^j \left(\frac{t_{fi}^j + t_{fo}^j}{2} - T_1^j\right) = \left(S_{p1}^j - S_{n1}^j\right) I T_1^j + K\left(T_1^j - T_2^j\right) - I^2 R_1^j/2 \tag{15}$$

$$h_2 A_2^j \left(T_2^j - \frac{t_{co}^j + t_{ci}^j}{2}\right) = \left(S_{p2}^j - S_{n2}^j\right) I T_2^j + K\left(T_1^j - T_2^j\right) - I^2 R_1^j/2 \tag{16}$$

As the temperature of fluid must be changed after heat transfer, therefore, the following equations can be obtained:

$$q_1^j = h_1 A_1^j \left(\frac{t_{fi}^j + t_{fo}^j}{2} - T_1^j\right) = \frac{C_f M_f \left(t_{fi}^j - t_{fo}^j\right)}{r} \tag{17}$$

$$q_2^j = h_2 A_2^j \left(T_2^j - \frac{t_{co}^j + t_{ci}^j}{2}\right) = \frac{C_c M_c \left(t_{co}^j - t_{ci}^j\right)}{r} \tag{18}$$

where C is the specific heat capacity, and M is the mass flow rate. t_f^j indicates the temperature of the exhaust gas and t_c^j is the temperature of the cooling air.

First, we assumed all units are independent and then divided the load resistance into n portions. Each portion is allotted to each PN couple, so we can calculate:

$$I = \frac{U^j}{\left(\frac{R_2}{n} + R_1^j\right)} = \frac{\left(S_{p1}^j - S_{n1}^j\right) T_1^j - \left(S_{p2}^j - S_{n2}^j\right) T_2^j}{\left(\frac{R_2}{n} + R_1^j\right)} \tag{19}$$

where R_2 is load resistance (external electric resistance), n is the total number of PN couples. It is seen that electric current I is still a function of T_1^j, T_2^j. Eqs. (15)–(19) constitute a complete problem to be solved with four unknowns of $t_{f0}^j, T_1^j, T_2^j, T_{co}^j$, as t_{fi}^j, t_{ci}^j is the initial value, or the value of last unit. However, an iteration calculation is needed. Accordingly, we can calculate the electric current I, and all the other unknown temperatures for each unit. As we know, the electric current I should be equal in a serial circuit; however, the obtained electric current I for each PN couple might be different. To resolve this issue, we sum up the currents of all portions, and then take an average. The averaged value is put back into the calculation until a tolerance is satisfied.

The output power of each PN couple can be expressed as:

$$P^j = \left(S_{p1}^j - S_{n1}^j\right) I T_1^j - \left(S_{p2}^j - S_{n2}^j\right) I T_2^j - I^2 R_1^j \tag{20}$$

and its efficiency can be given by:

$$\eta^j = P^j / q_1^j \tag{21}$$

The overall power output $P_{overall}$ and efficiency of power generation $\eta_{overall}$ can be obtained:

$$P_{overall} = r \sum_{j=1}^{m} P^j \tag{22}$$

$$\eta_{overall} = \sum_{j=1}^{m} P^j \Big/ \sum_{j=1}^{m} q_1^j \tag{23}$$

3. Results and discussion

Fig. 2a shows how the mass flow rate of exhaust gas varies for the federal test procedure (FTP-75) city driving cycle. Mass flow rate ranges from 5 g/s up to 45 g/s. Fig. 2b shows the variation in exhaust gas temperatures exiting the vehicle catalytic converter for the FTP-75 drive cycle [17]. The temperatures fluctuate around 500 °C, but do not fluctuate as much as the mass flow rates.

Table 1 lists the parameters for PN materials used in the present paper. The other parameters such as the temperature of the exhaust gas and convection heat transfer coefficient are listed in Table 2. In other subsequent analysis without special description, the parameters are taken from Tables 1 and 2.

Fig. 3 shows the calculation result of temperature profiles inside the TEG device with the parameters listed in Tables 1 and 2. The temperature of exhaust gas decreases from 500 °C to 383.7 °C; cooling-air temperature raises from 30 °C to 86.6 °C; temperature of semiconductor material ranges from 294.6 to 254.2 °C on the

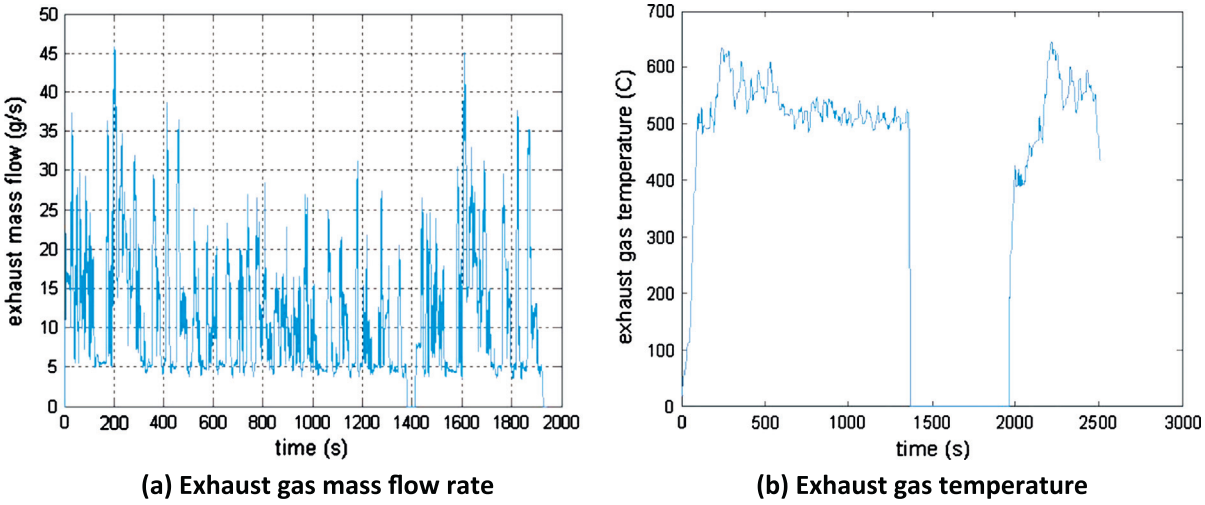

Fig. 2. Variation of exhaust gas mass flow rate and temperature with time for the FTP-75 drive cycle.

Table 1
Parameters of PN materials.

Parameters	P type	N type
Seebeck coefficient S^j	$40 + 0.20T$ (μV/K)	$40 + 0.20T$ (μV/K)
Electrical resistivity ρ^j	1.04×10^{-5} (Ωm)	1.04×10^{-5} (Ωm)
Thermal conductivity λ^j	1.5 (W/(mK))	2.5 (W/(mK))
Height H	0.005 (m)	0.005 (m)
Sectional area $A_p(A_n)$	0.01×0.01 (m^2)	0.01×0.01 (m^2)

Table 2
Other parameters.

Exhaust inlet temperature T_f	500 (°C)
Cooling-air temperature T_c	30 (°C)
Convection heat transfer coefficient of hot side h_1	100 (W/(m^2 K))
Convection heat transfer coefficient of cold side h_2	100 (W/(m^2 K))
Exhaust mass flow rate M_f	20 (g/s)
Cooling air mass flow rate of one side M_c	20 (g/s)
Ratio of external resistance to internal resistance R_2/R_1	1
Each unit's area A	0.015×0.025 (m^2)
Total area $A_{overall}$	0.15×0.5 (m^2)

Note: $R_1 = \sum_{j=1}^{n} R_1^j$.

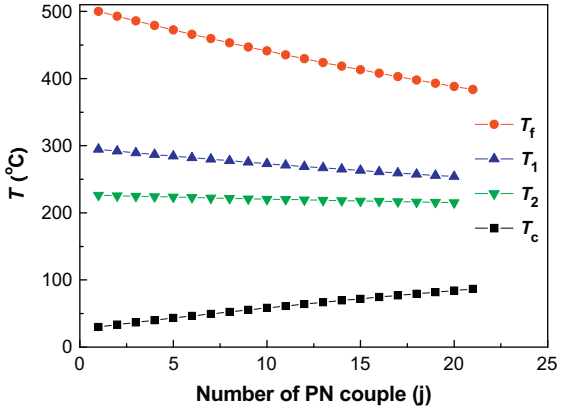

Fig. 3. Variation of temperatures of each unit for air-cooling.

hot side, while from 226.3 to 215.4 °C on the cold side; output power is 65.6 W; efficiency is 2.66%. We can conclude the utilization rate of waste heat of exhaust gas is quite low and directly manifested in the small temperature difference between inlet and outlet exhaust gas of the TEG. Although the efficiency of the thermoelectric is general low at the present stage, lower output power and efficiency are mainly caused by a low temperature difference between the hot side and cold side of the thermal material (which is almost 1/7 compared to the temperature difference between the exhaust gas and ambient air, as Fig. 3 shows. So, improving the coefficient of convective heat transfer of fluid from a heat transfer perspective, and developing new methods of thermoelectric transition from a thermodynamic perspective are quite necessary.

3.1. Effects of temperatures and mass flow rates of cooling-air

The variations of performance with temperatures and mass flow rates are shown in Fig. 4. Both the output power and efficiency decrease approximately linearly with the increment of cooling temperature. Because the rise in cooling temperature makes the temperature difference between the two sides of PN couple decrease, according to the Seebeck effect, resulting in the decrement of voltage, leading to the reduction of output power, we thus conclude that at lower cooling temperatures, the better the performance. With an increment of cooling-air mass flow rate, both the output power and efficiency increase nonlinearly. When the mass flow rate exceeds 40 g/s, the improvements of output power and efficiency are both quite small, while bigger mass flow rates always cost more power. There must be an optimal cooling mass flow rate value according to all parameters.

3.2. Effect of mass flow rates of exhaust gas

The variation of performance with exhaust gas mass flow rates is shown in Fig. 5. With an increment of exhaust gas mass flow rate, the output power and efficiency only increase noticeably when the mass flow rate is low; while the waste heat absorption of the TEG is insufficient when mass flow rate is high. Further, when the exhaust gas mass flow rate increases from 10 g/s to 30 g/s, output power increases only 20 W. If we use three of the same devices, we can get about 150 W output power, but it will definitely need larger volume and heavier weight.

3.3. Effects of convection heat transfer coefficient of each side

The variation of performance with convection heat transfer coefficient h_1 or h_2 is illustrated in Fig. 6. Along with either increase

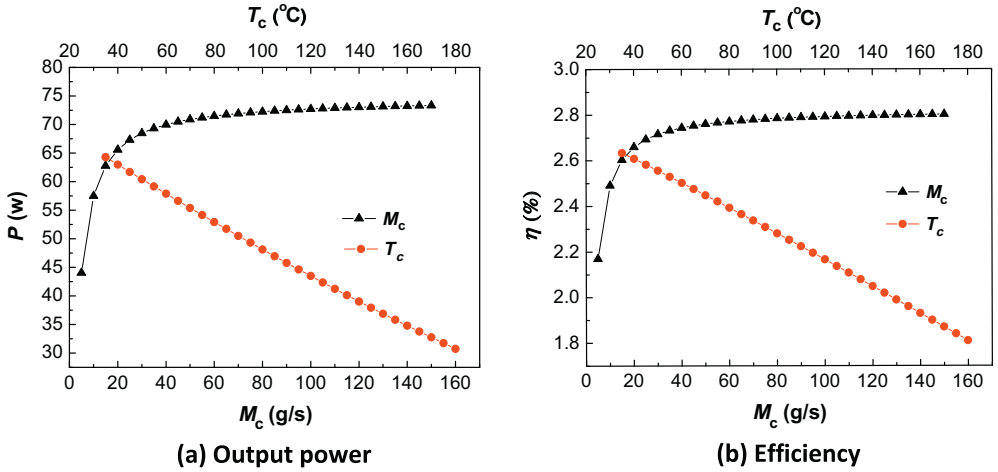

Fig. 4. Effects of temperature and mass flow rates of air-cooling on output power and efficiency.

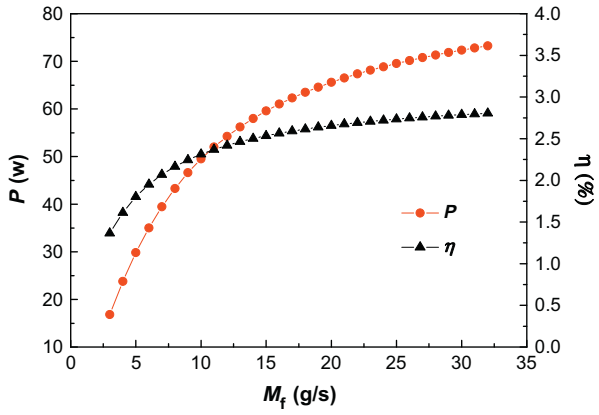

Fig. 5. Effect of mass flow rates of exhaust gas on power and efficiency.

h_1 or h_2, the output power and efficiency increases, but there are some differences. When h_1 or h_2 is very small, both the change trends of output power and efficiency are almost the same, growing rapidly. The normal triangular curve is slightly better than the circle dot curve when h_1 or h_2 is lower than 100 (W/m^2 K). However, as the convection heat transfer coefficient exceeds 100 (W/m^2 K), it begins to change significantly. The growth of output power and efficiency resultant from the increment of h_1 is still rapid, while the growth of output power and efficiency resultant from the increment of h_2 is slow. Although the temperature difference grows, the temperature of the hot side T_1 reduces with an increment of h_2. Considering the assumed Seebeck coefficient decreases with the decrement of temperature, so the improvements of output power and efficiency may be partially (even all) offset by a reduction of T_1. On the contrary, T_1 increases with the increment of h_1 and the temperature difference also grows, so it results in significant improvements of output power and efficiency. It is noted that the improvements of output power and efficiency will reduce rapidly if the temperature of the hot side T_1 is higher than the best working temperature range of the material.

In fact, it is much easier to enhance h_2 than h_1, such as using water-cooling instead of air-cooling. However, not enough improvement can be achieved by only increasing h_2.

3.4. Effect of height of the PN couple

The variation of performance with height of the PN couple is shown in Fig. 7. We can see that there must be an optimum H that maximizes the output power. When other parameters do not vary, the larger the H, the larger the temperature difference between the two sides of the TEG; however, H has a direct ratio relationship with internal resistance, and may reduce output power and efficiency.

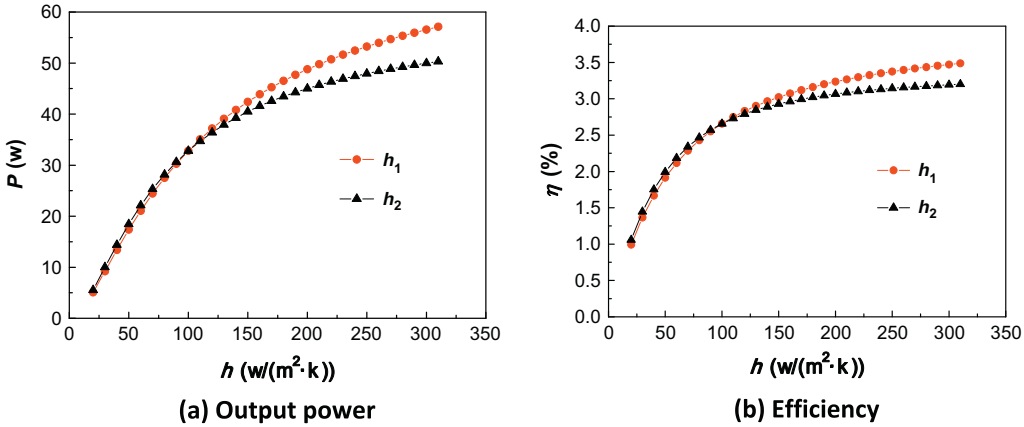

Fig. 6. Effects of convection heat transfer coefficient of either side on output power and efficiency.

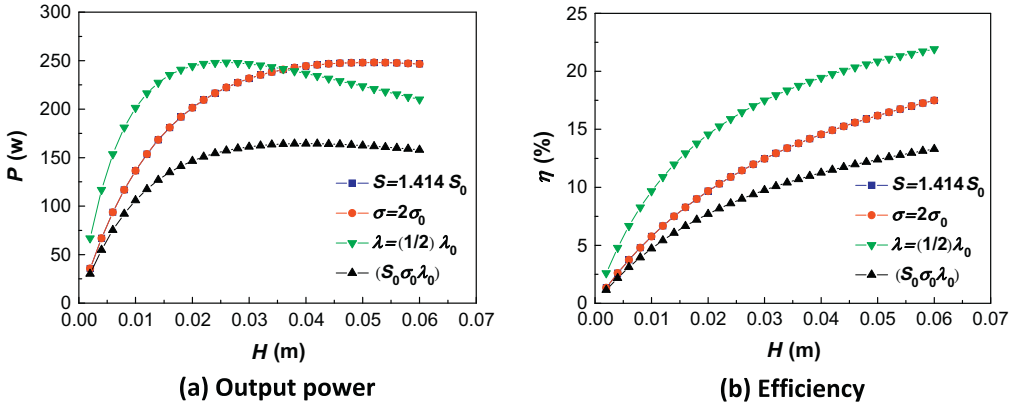

Fig. 7. Effect of height of PN couple on output power and Efficiency.

The dimensionless figure of *ZT* merit of semiconductor material can be defined as:

$$ZT = \frac{S^2\sigma}{\lambda}T \tag{24}$$

where T is the Kelvin temperature.

There are three ways to improve *ZT* value, as Eq. (24) shows, and will be analyzed respectively. When reducing λ, the best output power moves toward the direction of the reduction of H; while increasing the S or σ, the best output power moves toward to the direction of the increment of H, and those optimum output powers are nearly equal. All efficiencies increase with the increment of H. Generally speaking, a larger Seebeck coefficient S or electric conductivity σ results in a higher optimum H value; smaller thermal conductivity λ results in a smaller optimum H value. Moreover, higher height of material usually means higher cost in the same cross-sectional area condition, and will occupy more space and weight. Therefore, when we design a TEG device, we should choose an optimum H according to all parameters and economy. Just increasing the height of the material is not a good ideal to achieve greater output power and efficiency.

3.5. Effect of the ratio of external resistance and internal resistance

Fig. 8 shows the variation of performance with the ratio of external resistance to internal resistance. A maximum output power will occur at the ratio of about 1.5, as the normal triangular curve shows. This is different from a common electric circuit condition when external resistance is equal to internal resistance, because the generated voltage is influenced by current. Current decreases when resistance increases, causing the decrement of heat absorption or heat release of the Peltier effect, and causing the temperature increment difference of the two sides of the TEG, leading to voltage increases according to the Seebeck effect. Same analysis is done for the *ZT* value. We can conclude that the inverted triangle improves most than others, and the most likely reason is its H is far from the optimal value, so income is greatest. When H is near optimum value, the maximum output power may be almost equal. As shown in Fig. 8, we can conclude when we double *ZT* value in the three ways, best output power and efficiency all move toward the direction of the ratio increment, and the reduction of the λ condition moves most. Combined with 3.4, we have observed that the effect of S or σ is almost the same, while having some differences with the effect of λ for the performance of the TEG.

3.6. Comparison of different cooling-fluids

Considering that the convection heat transfer coefficient of air is smaller than that of water, the performance of the TEG using the engine cooling water as cooling fluid is investigated, and a comparison analysis is carried out with different cooling condition outcomes.

The vehicle engine cooling-water temperature is generally between 80 °C and 90 °C, so we assumed engine cooling-water, temperature, mass flow rate and coefficient of convective heat transfer respectively as 80 °C, 200 g/s and 1000 W/(m^2 K) (coefficient of the convective heat transfer of water is greater than air's in uniform conditions). As Fig. 9 shows, the temperature of exhaust gas decreases from 500 °C to 340.6 °C, otherwise water

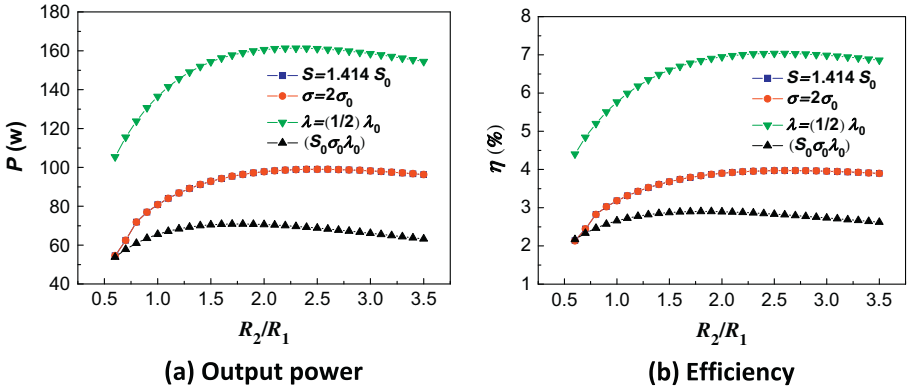

Fig. 8. Effect of the ratio of external resistance to internal resistance on output power and efficiency.

temperature raises from 80 °C to 87.7 °C, and the temperature of semiconductor material ranges from 213.4 to 166.5 °C on the hot side, and from 107.3 to 104.9 °C on the cold side. Output power is 113.3 W (improvement of 72.7% compared to air-cooling), and efficiency is 3.35%. Water-cooling is obviously better than air-cooling. Using the vehicle engine water coolant as the TEG's cooling-fluid to achieve water-cooling circulation is worthwhile in practical design and application.

3.7. Using phase-change material for heat transfer at the hot side

Combining Figs. 3 and 9, we can conclude that low coefficients of convective heat transfer (especially in exhaust pipe) are one of the important limiting factors on a TEG using vehicles exhaust as resource. Considering that backpressure of the engine must affect its efficiency, it is quite difficult to get significant improvement of the exhaust coefficient of convective heat transfer. As phase-change heat transfer has a huge coefficient, so we try to use phase-change material to reform our experiment's design. As Fig. 10 shows, phase-change fluid boils after absorbing heat from the gas in the exhaust pipe, then it condenses to liquid after releasing heat to the hot side of the TEG. The condensate liquid flows to the boiling side, moving cyclical. Fig. 11 shows the comparison of output power and efficiency between a system using phase-change material and a normal heat convection system (we assume the phase-change heat transfer coefficient of exhaust is 5000 W/(m^2 K), while the cooling water coefficient of convective heat transfer is 1000 W/(m^2 K), and the cooling-water's inlet temperature is 80 °C, and mass flow rate is 200 g/s).

Using material with lower phase-change temperature (than exhaust gas) must reduce the "quality" of exhaust waste heat, but a huge heat transfer phase-change coefficient still brings significant improvement of both output power and efficiency, as Fig. 11 shows. Circle dot is the calculation result using phase-change material. We can conclude that output power improves greater than 10 times at 45 g/s mass flow rate and of over 165% at 5 g/s mass flow rate, while efficiency improves greater than 148% at 45 g/s mass flow rate, and of over 313% at 5 g/s mass flow rate for the system using phase-change material versus the normal system. The comparisons of exhaust outlet temperature of the TEG with different mass flow rates for those two systems are shown in Fig. 12. We observe that when mass flow rates are below 35 g/s, the exhaust outlet temperatures of the TEG are equal to 300 °C. This means the heat absorbed by the phase-change fluid is finite, only part of PN couples are working (the influence between PN couples is not discussed in this paper), output power increases greatly with flow rate increases. The outlet temperature of cooling-water also increases, so the efficiency decreases slightly. When flow rates of exhaust are beyond 35 g/s, the output power of the TEG reaches a maximum value, and increasing the flow rate does not have influence on output power and efficiency, while the exhaust outlet temperature of the TEG increases. This is because, limited by the dimension of the TEG device, the heat absorption capacity of the TEG reaches maximum, all PN couples are working within large temperature differences.

Without question, if we use material with a 300 °C phase-change temperature, the process from 500 °C to 300 °C must reduce the "quality" of waste exhaust heat, and if we choose material with a higher phase-change temperature, we therefore cannot

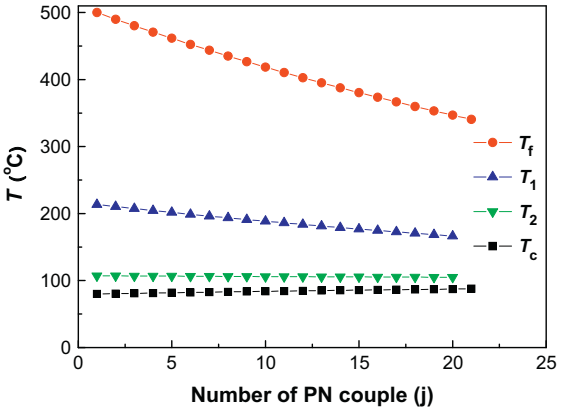

Fig. 9. Temperatures of each unit under water-cooling condition.

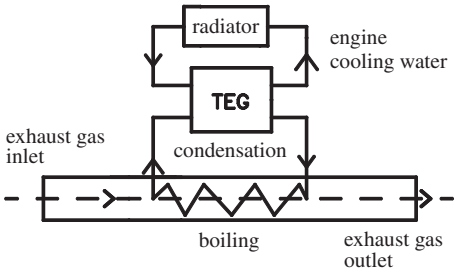

Fig. 10. Simple systematic diagram using phase-change material.

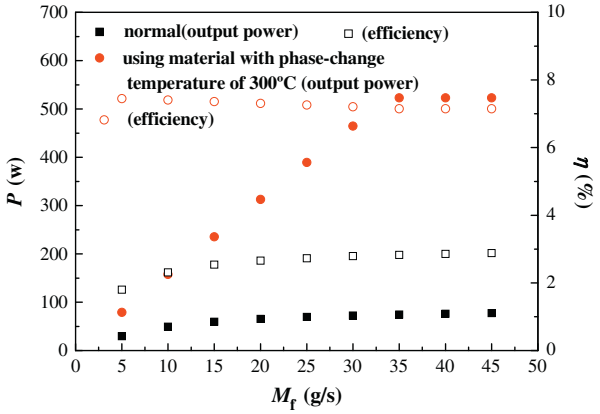

Fig. 11. Comparison of output power and efficiency under phase-change condition and normal condition.

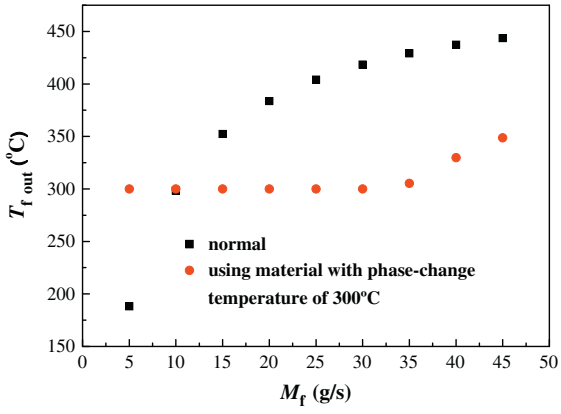

Fig. 12. Variation of outlet temperature of the TEG device for different mass flow rates of exhaust gas.

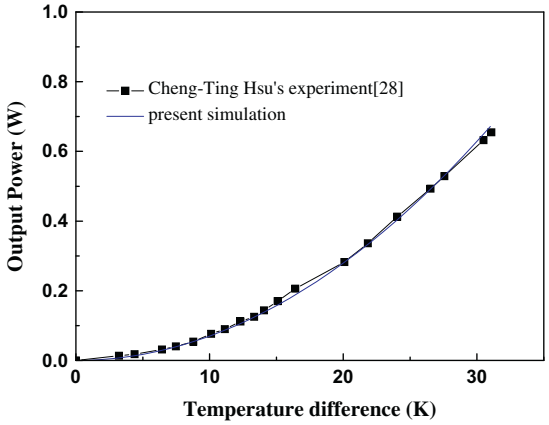

Fig. 13. Comparison of present simulation result and experimental result in literature.

recover exhaust water heat below the phase-change temperature. It will not be a small loss. So we put forward to a new idea using a two-stage (or more) combination of materials with different phase-change temperatures, along the flowing direction of exhaust gas for cascade utilization of exhaust waste heat to remit this problem. Detailed analysis of this ideal will be reported in another paper.

In fact, in the circumstance using phase-change materials to improve the output power and efficiency of the TEG, it is not enough to consider just the temperature of the phase-change materials and phase change heat transfer coefficient. The heat convection coefficient between the exhaust gas and evaporator is also an important influencing factor. In the analysis of this paper, it is assumed the heat exchange surface between the exhaust gas and evaporator is large enough, compared to that of a semiconductor generator. So the influence of the boiling heat transfer coefficient of phase-change materials and the convection heat transfer coefficient between the exhaust gas and the evaporator can be ignored.

3.8. Comparison of the present simulation result and experimental result in literature

In order to verify the validity of the model in this paper, the present simulation result and the experimental result in literature [29] are compared, as shown in Fig. 13, with abscissa for temperature difference and ordinate as output power. As can be seen in the temperature range shown in the figure, good agreement exists with those obtained in this paper, so the model calculation results are reliable.

4. Conclusion

Based on Fourier's law and the Seebeck effect, this paper presents a mathematical model of a Thermoelectric Generator (TEG) device using the exhaust gas of vehicles as heat source, and preliminary analysis of the impact of relevant factors on the output power and efficiency of the TEG. Main conclusions are as follows:

(1) In an air-cooling condition, the increasing convection heat transfer coefficient of either side of the TEG will result in output power and efficiency increases, but the effects are different. The change trends of the output power and efficiency are roughly the same when the heat transfer coefficient is small. When either convection heat transfer coefficient exceeds the other, the improvements of output power and efficiency by the increment of convection heat transfer coefficient of the high-temperature-side are greater than by the increment of convection heat transfer coefficient of the low-temperature-side. But, because of the limited space and backpressure of the exhaust, the increment of convection heat transfer coefficient of the high-temperature-side is quite difficult or costly.

(2) With the change of height of the PN couple, there is a peak value of output power. This best height value for peak point decreases with the decrement of thermal conductivity of material, and increases with the increment of the Seebeck coefficient and electric conductivity of the material.

(3) The output power and efficiency of the TEG change with the change of the ratio of external resistance to internal resistance, and there also exists a maximum. The maximum value appears when the external resistance is greater than the internal resistance. It is different from a common circuit at the time the external resistance is equal to internal resistance. And with the increment of the *ZT* value, the maximum value ratio moves toward the direction of increasing the ratio of external resistance to internal resistance.

(4) A preliminary analysis of the possibility of using phase-change materials to reinforce the heat transfer property of the high-temperature-side of the TEG was carried out, and the results show that using appropriate phase-change materials can significantly improve the output power and efficiency of the TEG.

Acknowledgment

The authors are grateful to the financial support by the National Fundamental Research Program of China (*2011CB707203*).

References

[1] Yu C, Chau KT. Thermoelectric automotive waste heat energy recovery using maximum power point tracking. Energy Convers Manage 2009;50:1506–12.
[2] Stabler F. Automotive applications for high efficiency thermoelectrics. In: High efficiency thermoelectric workshop; 2002.
[3] Mori M, Yamagami T, Oda N, Hattori M, Sorazawa M, Haraguchi T. Current possibilities of thermoelectric technology relative to fuel economy. Soc Autom Eng 2009;2009:01–0170.
[4] Vazquez J, Sanz-Bobi M, Palacios R, et al. State of the art of thermoelectric generators based on heat recovered from the exhaust gases of automobiles. In: Proceedings of the seventh European workshop on thermoelectrics; 2002.
[5] Gou XL, Xiao H, Yang SW. Modeling, experimental study and optimization on low-temperature waste heat thermoelectric generator system. Appl Energy 2010;87(10):3131–6.
[6] Department of Energy; July 2010. <http://www.energy.gov/energyefficiency/index.htm>.
[7] Fairbanks J. Thermoelectric applications in vehicles status 2008. In: Proceedings of the 6th European conference on thermoelectrics, ICMPE-CRNS; 2008. p. 1–8.
[8] Bell LE. Cooling, heating, generating power, and recovering waste heat with thermoelectric systems. Science 2008;321:1457–61.
[9] Boukai AI, Bunimovich Y, Tahir-Kheli J, et al. Silicon nanowires as efficient thermoelectric materials. Nature 2008;451:168–71.
[10] Hochbaum AI, Chen RK, Delgado RD, et al. Enhanced thermoelectric performance of rough silicon nanowires. Nature 2008;451:163–7.
[11] Heremans JP, Jovovic V, Toberer ES, et al. Enhancement of thermoelectric efficiency in PbTe by distortion of the electronic density of states. Science 2008;321:554–7.
[12] Hsu KF, Loo S, Guo F, et al. Cubic AgPbmSbTe2+m: bulk thermoelectric materials with high figure of merit. Science 2004;303:818–21.
[13] Xiao JS, Yang TQT, et al. Thermal design and management for performance optimization of solar thermoelectric generator. Appl Energy 2012;93:33–8.
[14] Rowe DM, Gao M. Design theory of thermoelectric modules for electrical power generation. IEE Proc Sci Meas Technol 1996;143(6):351–6.
[15] Hsu CT, Huang GY, Chu HS, et al. An effective Seebeck coefficient obtained by experimental results of a thermoelectric generator module. Appl Energy 2011;88:5173–9.
[16] Liang GW, Zhou JM, Huang XZ. Analytical model of parallel thermoelectric generator. Appl Energy 2011;88:5193–9.
[17] Hsiao YY, Chang WC, Chen SL. A mathematic model of thermoelectric module with applications on waste heat recovery from automobile engine. Energy 2010;35:1447–54.

[18] Kim S. Analysis and modeling of effective temperature differences and electrical parameters of thermoelectric generators. Appl Energy 2012.
[19] Crane DT, Bell LE. Design to maximize performance of a thermoelectric power generator with a dynamic thermal power source. J Energy Resour Technol Trans ASME 2009;131:11–8.
[20] Eakburanawat J, Boonyaroonate I. Development of a thermoelectric battery-charger with microcontroller-based maximum power point tracking technique. Appl Energy 2012;83:687–704.
[21] Espinosa N. Modeling a thermoelectric generator applied to diesel automotive heat recovery. J Electron Mater 2010;39:1446–55.
[22] Chen LG, Sun FR, Wu C. Thermoelectric-generator with linear phenomenological heat-transfer law. Appl Energy 2005;81:358–64.
[23] Chen LG, Li J, Sun FR, et al. Performance optimization of a two-stage semiconductor thermoelectric-generator. Appl Energy 2005;82:300–12.
[24] Salzgeber K, Prenninger P, Grytsiv A, et al. Skutterudites: thermoelectric materials for automotive applications? J Electron Mater 2010;39:2074–8.
[25] Takanose E, Tamakoshi H. The development of thermoelectric generator for passenger car. In: Proceedings of the 12th IEEE international conference on thermoelectrics; 1993. p. 467–70.
[26] Ikoma K, Munekiyo M, Furuya K, et al. Thermoelectric generator for gasoline engine vehicles using Bi_2Te_3 modules. Jpn Inst Met 1999;63(11):1475–8.
[27] Thacher E, Helenbrook B, Karri M, et al. Testing of an automobile exhaust thermoelectric generator in a light truck. Proc Inst Mech Eng D J Auto Eng 2007;221:95–107.
[28] Schlichting A, Anton S, Inman D. Motorcycle waste heat energy harvesting. In: Proceedings of the SPIE industrial and commercial applications of smart structures technologies; 2008. p. 6930.
[29] Hsu CT, Huang GY, Chu HS, et al. Experiments and simulations on low-temperature waste heat harvesting system by thermoelectric power generators. Appl Energy 2011;88:1291–7.
[30] Hsu CT. Renewable energy of waste heat recovery system for automobiles. J Renew Sustain Energy 2010;2:013105 (12pp).
[31] Masahide M, Michio M, Masaru O. Thermoelectric generator utilizing automobile engine exhaust gas. Therm Sci Eng 2001;9:17–8.
[32] Yodovard P. The potential of waste heat thermoelectric power generation from diesel cycle and gas turbine cogeneration plants. Energy Source 2001;23:213–4.
[33] Xu LZ, Li Y, Yang Z, et al. Experimental study of thermoelectric generation from automobile exhaust. J Tsinghua Univ (Sci Technol) 2010;50(2):287–9. 94.
[34] Zhang YP, Hu HP, Kong XD, et al. Energy storage of phase-change. Hefei: Chinese Science and Technology University Press; 1996.
[35] Suter C, Jovanovic ZR, et al. A 1 kW thermoelectric stack for geothermal power generation – modeling and geometrical optimization. Appl Energy 2012;99:379–85.
[36] Zhang XD, Chau KT. Design and implementation of a new thermoelectric photovoltaic hybrid energy system for hybrid electric vehicles. Electr Power Compon Syst 2011;39:511–25.
[37] van Sark WGJHM. Feasibility of photovoltaic – thermoelectric hybrid modules. Appl Energy 2011;88:2785–90.
[38] Qiu K, Hayden A. Integrated thermoelectric and organic Rankine cycles for micro-CHP systems. Appl Energy 2012;97:667–72.
[39] Pan YZ, Lin BH, et al. Performance analysis and parametric optimal design of an irreversible multi-couple thermoelectric refrigerator under various operating conditions. Appl Energy 2007;84:882–92.
[40] Chen WH, Chen YL, et al. A numerical study on the performance of miniature thermoelectric cooler affected by Thomson effect. Appl Energy 2012;89:464–73.
[41] Cheng CH, Huang SY. Development of a non-uniform-current model for predicting transient thermal behavior of thermoelectric coolers. Appl Energy 2012;100:326–35.
[42] Chatterjee S, Pandey KG. Thermoelectric cold-chain chests for storing/transporting vaccines in remote regions. Appl Energy 2003;76:415–33.